ELSEVIER

Surface Science 491 (2001) 48–62

SURFACE SCIENCE

www.elsevier.com/locate/susc

Tuning the chemistry of metal surfaces: I. Adsorption and reaction of NO and N_2O on ultrathin Pd films on Ta(1 1 0)

David E. Beck [a], John M. Heitzinger [a,b], Armen Avoyan [a,c], Bruce E. Koel [a,*]

[a] *Department of Chemistry, University of Southern California, Los Angeles, CA 90089-0482, USA*
[b] *FSI International, 322 Lake Hazeltine Drive, Chaska, MN 55318-1096, USA*
[c] *Lam Research Corp, 4650 Cushing Parkway, Fremont, CA 94538, USA*

Received 28 December 2000; accepted for publication 29 May 2001

Abstract

Nitric oxide (NO) chemisorption is a sensitive chemical probe of the electronic structure and reactivity of metal surfaces. We have used NO, in conjunction with temperature programmed desorption and high resolution electron energy loss spectroscopy, to explore the altered reactivity of ultrathin (monolayer, bilayer, trilayer) Pd films deposited on Ta(1 1 0). The reactivity of the Pd-monolayer film is strongly altered from that of bulk-terminated Pd surfaces. NO is molecularly adsorbed on the Pd monolayer at 95 K, but the desorption activation energy is decreased to only 8 kcal/mol, and N_2O is the primary desorption product. At low initial NO coverages, N_2O desorbs in a reaction rate-limited peak at 129 K, which grows and shifts up in temperature, with increasing coverage, to 159 K at saturation. NO desorption occurs at 135 K, in addition to N_2O, at high coverages. Separate N_2O adsorption experiments show that N_2O is weakly and reversibly bound to the Pd monolayer film, desorbing by 115 K. NO chemisorption and reaction was independent of the initial geometric structure of the Pd monolayer, i.e., nearly identical results were obtained when using a pseudomorphic-bcc(1 1 0) or incommensurate-fcc(1 1 1) Pd monolayer. However, the chemical properties and reactivity of the Pd films rapidly returned to that of bulk Pd(1 1 1) surfaces as the Pd film thickness was increased above one monolayer. "Tuning" of NO chemistry on these Pd films was possible for initial thicknesses of 2–3 layers. The interaction of NO with a Pd monolayer on Ta(1 1 0) closely resembles that of NO with a Ag(1 1 1) surface, supporting the interpretation that Pd–Ta bonding interactions lead to a filled Pd d-band resulting in more noble metal-like properties.

Keywords: Electron energy loss spectroscopy (EELS); Thermal desorption spectroscopy; Catalysis; Thermal desorption; Palladium; Tantalum; Nitrogen oxides; Single crystal surfaces; Metallic films

1. Introduction

The chemisorption properties of monolayer and ultrathin (bilayer, trilayer, etc.) films of Pd on refractory metal substrates are very different from those of bulk-terminated Pd surfaces. This was discovered by investigations that explored the interaction of H_2 [1–6] and CO [1–4,7–13] with such Pd films. These studies showed that H_2 and CO chemisorption was much weaker on a Pd monolayer than on thick Pd films. However, H_2 and CO chemisorption do not nearly give a complete description of the reactivity of these ultrathin Pd

* Corresponding author. Tel.: +1-213-740-7036; fax: +1-213-740-2701/746-4945.
E-mail address: koel@chem1.usc.edu (B.E. Koel).

0039-6028/01/$ - see front matter
PII: S0039-6028(01)01321-8

films, and we are motivated to make further investigations of the chemisorption and reaction of other appropriate probe molecules to explore and help elucidate the underlying reasons for the altered chemisorption properties of these films.

Ultrathin films of Pd on refractory metal substrates have a very different electronic structure from that of bulk Pd samples. This was shown originally in ultraviolet photoelectron spectroscopy (UPS) spectra from Pd/Nb(1 1 0) and Pd/Ta(1 1 0), which showed a reduced density-of-states (DOS) at the Fermi energy (E_f), and an attenuation and shift to higher binding energy of the 4d band [14–18]. The origin of this difference was originally interpreted as the complete filling of the Pd 4d band [19]. This could occur by charge transfer from the substrate to Pd and/or by substrate-induced rehybridization of the Pd valence orbitals (s to d conversion). However, X-ray photoelectron spectroscopy (XPS) measurements for Pd monolayers on Ta(1 1 0) [20] showed a shift of the Pd (3d) core levels to higher binding energy when compared to the surface atoms of Pd(1 0 0), and this shift was attributed to charge transfer from the Pd overlayer to the substrate, creating a partial positive charge on the Pd atoms in the monolayer [21]. It was argued that there was a lower Pd 4d electron density in the Pd monolayer than at bulk Pd surfaces. The difficulties in understanding core-level shifts in XPS are well known, and considerable debate could surround this issue for some time [22]. For example, Pd s-to-d rehybridization could also cause core-levels to shift to higher binding energy (because valence s electrons screen the nucleus more effectively than valence d electrons), and final state effects in XPS [23] make it difficult to interpret small XPS shifts. In addition, the Ta (4f) surface core-levels also shift toward higher binding energy upon Pd deposition [24], which is contrary to the result expected within the framework of a simple charge-transfer model.

Probing the chemistry of these Pd films using different molecules offers a supplemental approach to these difficult spectroscopic problems. Previously, we have investigated the chemisorption properties of H_2 [6] and CO [12] on Pd/Ta(1 1 0). Acetylene and benzene chemisorption, along with the acetylene-cyclotrimerization reaction, was also explored on Pd/Ta(1 1 0), and these results will be reported separately. In the present paper, we discuss nitric oxide (NO) chemisorption studies on ultrathin Pd films on Ta(1 1 0). A brief study of N_2O adsorption was also made because we observed N_2O as a reaction product in the NO experiments.

NO is a versatile probe molecule, in part, because NO is a weaker π-acid (π-acceptor) than CO and probes different parts of the electron density during chemisorption on metals. NO is also a much more sensitive and versatile ligand than CO because of its singly occupied $2\pi^*$ orbital and thus resultant possibilities for covalent bonding. NO bonds in both linear and bent geometries on atop sites [25–28] or bridging sites [26–30], or in a "lying down" configuration [31]. The weaker molecular bond in NO compared to that in CO also leads to more facile dissociation and reaction on late transition metal surfaces, such as on Ag where low temperature reactions form N_2O [32–34]. Thus, NO enables probing the Pd-monolayer and thin film chemistry with more sensitivity than with CO. Additionally, information on how surface reactivity is controlled by Pd film structure and thickness may aid in catalyst development for reducing NO_x emissions from internal-combustion engine exhaust.

2. Experimental information

The UHV apparatus used in this study has been described previously [35]. The instrumentation on the chamber included a double-pass CMA with a coaxial electron gun, LEED optics, UTI 100C quadrupole mass spectrometer and high resolution electron energy loss spectroscopy (HREELS) spectrometer. The base pressure of the chamber was 1×10^{-10} Torr.

The Ta(1 1 0) single crystal was cleaned by Ar^+ ion sputtering followed by repeated flashes to 2500 K in UHV. The temperature of the sample was measured by a W-5%Re/W-26%Re thermocouple spotwelded to the side of the sample. Pd was deposited on the Ta(1 1 0) surface by resistively heating a 0.5-mm W wire which was wrapped with 0.1-mm Pd wire (Aesar, 99.99% pure).

NO (Matheson, CP grade) was passed through a dry ice–methanol trap prior to dosing. N_2O (MG Industries, 99.9%) was used without any further purification. Dosing of all gases was carried out using a glass microcapillary array doser attached to a leak valve, with a flux enhancement factor of 50 over the measured background pressure. Exposures are reported in units of Langmuirs ($1\ L = 1 \times 10^{-6}$ Torr s) and the values given in this paper have been corrected for ionization gauge efficiency and doser enhancement factor. NO coverage was determined by temperature programmed desorption (TPD) peak areas from a saturation NO dose on a thick ($\theta_{Pd} = 5$) film. The TPD peak profile from this experiment reproduced the results from a bulk-terminated Pd(1 1 1) surface which has a saturation NO coverage of 0.75 ML.

The heating rate used during TPD experiments was 5 K/s. HREELS was performed in the specular direction with an incident electron beam energy of 4 eV. The resolution of the spectrometer varied between 60 and 85 cm^{-1}, and all spectra were recorded with a substrate temperature of $T \leqslant 100$ K.

The growth and structure of Pd films formed by vapor-deposition on Ta(1 1 0) has been studied previously [4,8,36,37]. At 300 K, growth is by a Frank-van der Merwe (layer-by-layer) mechanism. The first Pd layer grows in a two-dimensional, pseudomorphic structure up to $\theta_{Pd} = 0.65$ (defined relative to the atomic density of the (1 1 1) surface of bulk Pd, 1.53×10^{15} cm^{-2} for $\theta_{Pd} = 1$). Subsequent deposition of Pd causes a "beat" pattern [37] to appear in LEED with the new spots aligned parallel to the short axis of the distorted hexagonal pattern of the bcc(1 1 0) substrate. The beat pattern indicates the onset of a structural phase-transition and has been attributed to the formation of fcc(1 1 1) islands [36,38,39]. Further deposition, up to $\theta_{Pd} = 1$, leads to the formation of an fcc(1 1 1) *incommensurate* Pd monolayer. As the Pd film thickness is increased above a monolayer, the beat pattern observed in LEED fades and a symmetric hexagonal pattern appears that is characteristic of an fcc(1 1 1) structure. The growth of Pd films on Ta(1 1 0) at 125 K is characterized by AES intensities that are nearly identical to those for growth at 300 K, indicating similar film growth and structure.

Regarding the thermal stability of these films, the bcc(1 1 0) pseudomorphic Pd monolayer is stable to 1350 K, but the fcc(1 1 1) incommensurate Pd monolayer is stable only to temperatures of 550–600 K. The beat pattern in LEED disappears at these temperatures and a (1×1) pattern is seen due to the formation of a pseudomorphic Pd monolayer structure with $\theta_{Pd} = 0.86$. Thicker films are less stable, and agglomerate into three dimensional structures that are two- or three-layers thick at temperatures as low as 370 K. Specifically for a Pd bilayer ($\theta_{Pd} = 2$) film, the Pd AES signal sharply decreases after annealing to 350–450 K and has only 85% of the initial intensity after heating to 850 K. This has been attributed to the formation of Pd clusters with an average thickness estimated at two layers [36]. Heating to 550–600 K, causes the beat pattern to disappear and a new pattern to form with elongated spots. This new pattern changes at about 850 K to a (1×1) pattern. The new LEED pattern has been associated with two- or three-layer thick Pd clusters, with a structure close to that of a bulk-terminated Pd(1 0 0) crystal, on top of the pseudomorphic Pd monolayer on Ta(1 1 0). This structure induces only a 4% lattice strain in the Pd clusters compared to the 20% lattice strain in the [1 1 0] direction of the pseudomorphic structure. For Pd films with $\theta_{Pd} = 3$, the beat pattern disappears at 650 instead of 600 K, but otherwise the changes that occur in the Pd and Ta AES intensities from annealing are similar to those for $\theta_{Pd} = 2$.

Pd coverages reported in this paper were derived from AES and LEED observations [36]. NO coverages were estimated by comparing the thick film NO desorption peak areas to those from known coverages on a Pd(1 1 1) bulk terminated surface. All of the NO and N_2O adsorption experiments were performed on Pd films that were preannealed to 600 K, unless otherwise specified, in order to minimize changes in the Pd film structure during subsequent TPD experiments or annealing studies of NO adlayers. For the $\theta_{Pd} = 1$ film experiments, the annealing conditions prior to gas dosing did not remove the beat pattern in LEED that is

characteristic of the fcc(1 1 1) Pd monolayer structure.

3. Results

3.1. NO adsorption on a fcc(1 1 1)-Pd monolayer, $\theta_{Pd} = 1$

3.1.1. Temperature programmed desorption

Fig. 1 shows TPD spectra for NO and N_2O desorption after NO exposures on a $\theta_{Pd} = 1$ film at 95 K. A desorption peak occurs at 129 K in the NO spectra (Fig. 1a) at low initial NO exposures, which grows and shifts up in temperature as the NO exposure is increased, finally saturating at 159 K. NO desorption for this series of peaks is coincident with N_2O desorption throughout the entire range of NO exposures and we attribute this signal to cracking of an N_2O product in the QMS ionizer rather than to NO desorption. NO desorption at 135 K, and high initial NO exposures, has no counterpart in the N_2O spectrum and so is clearly due to molecular NO desorption. The NO desorption activation energy E_d can be estimated to be 8 kcal/mol by Redhead analysis [40] assuming first-order kinetics and a preexponential of 10^{-13} s^{-1}.

N_2O was the primary desorption product in TPD following NO exposures as shown in Fig. 1b. N_2O desorbs in a peak at 129 K at low NO exposures, that increases in size and shifts up to 159 K as the peak saturates. Separate N_2O desorption experiments show that N_2O desorption occurs in a reaction rate-limited process, and thus the activation energy of these reactions can be estimated to be 10 kcal/mol.

These results can be contrasted with NO adsorption and desorption from the (1 1 1) surface of a bulk Pd single crystal. For comparison, Fig. 2 reproduces previous TPD results after NO exposures on Pd(1 1 1) at 100 K [27]. At low coverages, NO desorbs in a high temperature peak at 540 K. With increased coverage, this peak shifts slightly to lower temperatures and new peaks appear at 290 and 270 K. Values for E_d corresponding to these three peaks were estimated to be 38, 21 and 20 kcal/mol, respectively [27]. Adsorption wasc ompletely reversible; no desorption products other than NO were observed and no decomposition of NO occurred.

The chemistry of NO on the fcc(1 1 1)-Pd monolayer film is dramatically altered. The reaction of NO to form N_2O is the dominant thermal pathway and all NO desorption occurred below

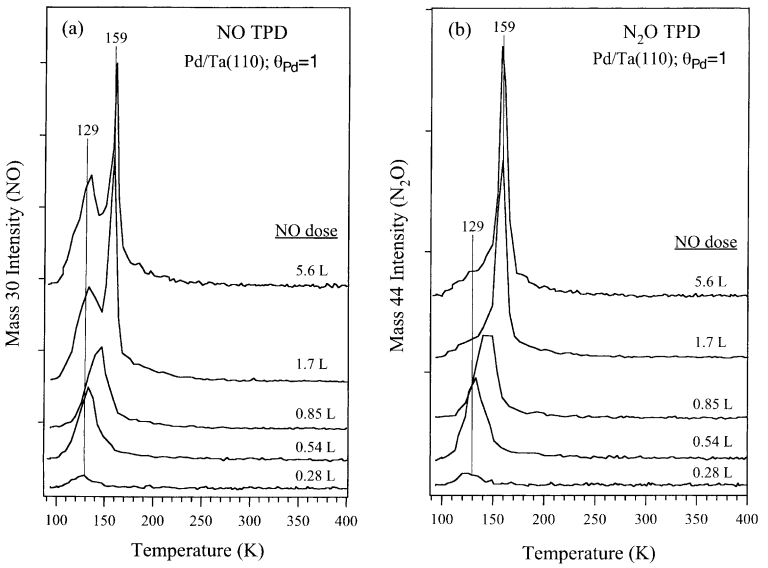

Fig. 1. TPD spectra after NO exposures on a $\theta_{Pd} = 1$ film at 95 K: (a) NO TPD spectra (30 amu) and (b) N_2O TPD spectra (44 amu).

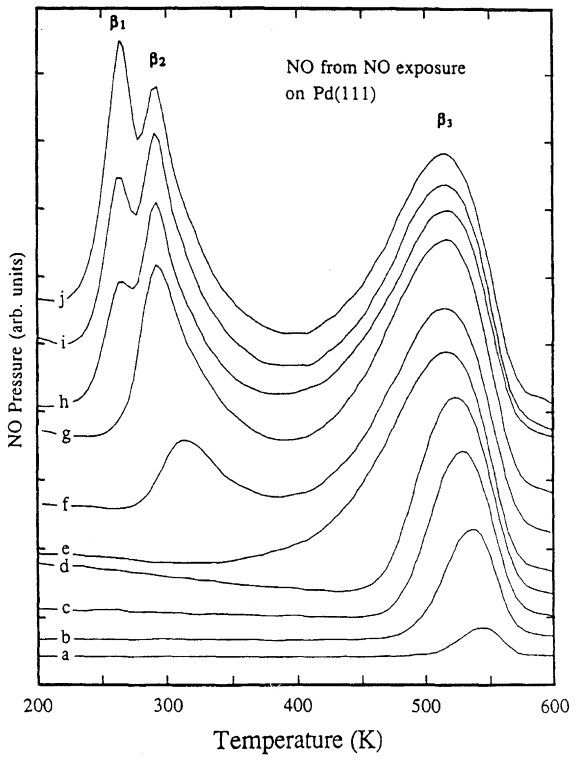

Fig. 2. NO TPD spectra after NO exposures on a Pd(1 1 1) single crystal at 100 K.

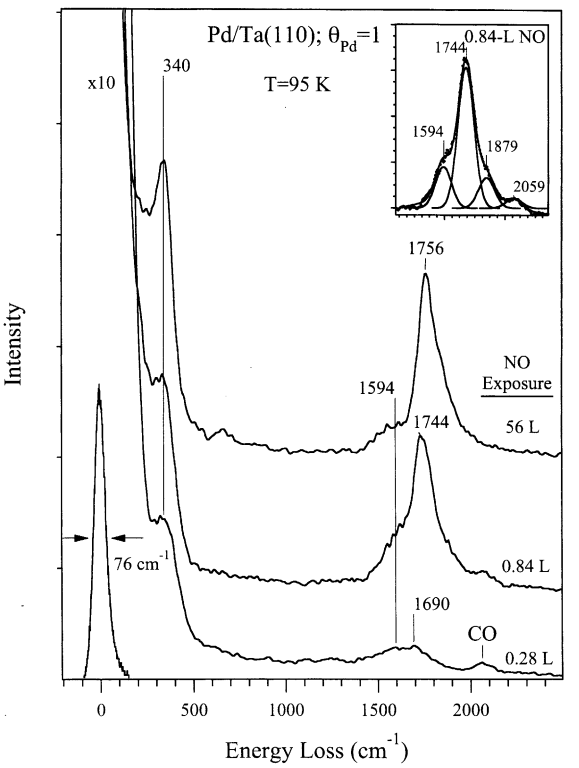

Fig. 3. HREELS spectra following NO exposures on a $\theta_{Pd} = 1$ film at 95 K. The inset shows a decomposition of the feature at 1744 cm^{-1} into contributions from several components.

250 K. Molecular NO desorption accounts for only ~16% of adsorbed NO and there is a strong reduction in the NO chemisorption bond energy relative to even the most weakly bound states of NO on bulk-terminated Pd(1 1 1) surfaces.

3.1.2. High resolution electron energy loss spectroscopy

Vibrational studies using HREELS were conducted to characterize the nascent species formed by NO adsorption on the fcc(1 1 1)-Pd monolayer at 95 K. Fig. 3 shows some of these results. Loss peaks near 340, 1594, and 1690 cm^{-1} were observed after a small, 0.28-L NO exposure. Larger exposures produced a broad, structured feature with a peak at 1744 cm^{-1}. The inset in Fig. 3 provides a decomposition of this feature into four components at 1594, 1744, 1879 and 2059 cm^{-1}. Later, we assign these peaks to NO bonded in bridge sites, the asymmetric and symmetric NO stretching bands of an adsorbed NO dimer $(NO)_2$, and to coadsorbed CO, respectively.

As shown in Fig. 4, heating the surface to 125 K after an initial exposure of 0.28-L NO eliminated all loss peaks, which is consistent with the TPD results. This exposure produced a coverage of ~15% of a monolayer.

Little change is caused by heating a monolayer coverage to 125 K. Fig. 5 shows that annealing to 150 K caused the disappearance of the 1744 cm^{-1} feature, leaving a small broad peak at 1648 cm^{-1}. NO and N_2O evolution occur in TPD near this temperature. Heating to 175 K reduces the intensity of the 1648 cm^{-1} loss peak, and annealing to 250 K leaves only small peaks at 358 and 682 cm^{-1}. These latter peaks are due to oxygen (or possibly nitrogen) adatoms because N and O signals were detected subsequently by AES. However, the chemical environment is different from that on

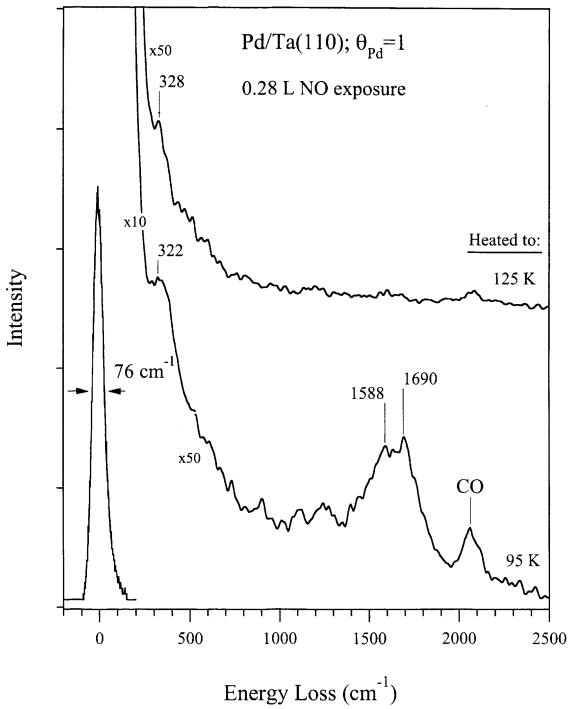

Fig. 4. HREELS spectra following a 0.28-L NO exposure on the Pd monolayer at 95 K, and after annealing to 125 K.

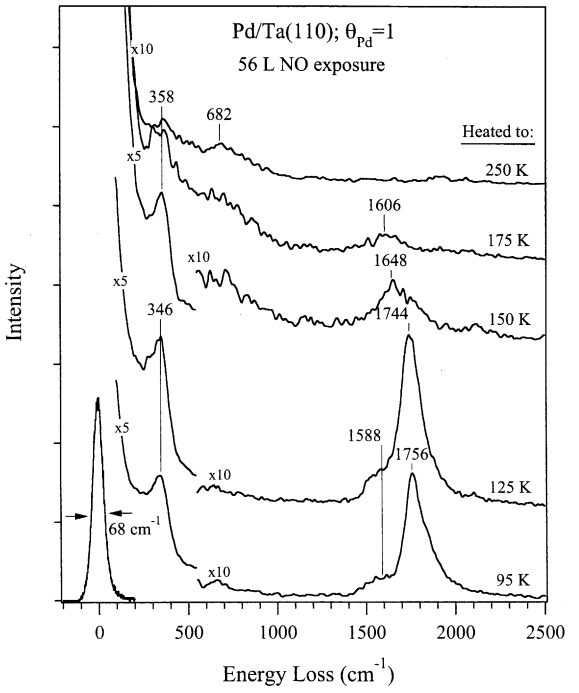

Fig. 5. HREELS spectra after a 56-L NO exposure on the Pd monolayer at 95 K followed by annealing to the specified temperature.

bulk Pd(1 1 1) where chemisorbed oxygen has a peak at 475 cm^{-1} and oxidation produces a broad feature at 510 cm^{-1} [21].

These results can be contrasted with HREELS spectra for NO adsorbed on a bulk-terminated Pd(1 1 1) sample [27]. Fig. 6 shows that low coverages ($\theta_{NO} = 0.26$) are characterized by a single peak at 1570 cm^{-1} that has been assigned to NO occupying twofold bridge sites. Peaks occur at 1595 and 1735 cm^{-1} with nearly equal intensities at monolayer coverage. The peak at 1735 cm^{-1} has been attributed to NO coordinated at atop sites. Also, HREELS spectra following a small, 0.28-L NO exposure on a thick, $\theta_{Pd} = 5$ film at 95 K showed a single peak at 1558 cm^{-1}, which is similar to that on bulk Pd(1 1 1). NO adsorption and bonding on a $\theta_{Pd} = 5$ film at 95 K corresponds well to that on a bulk Pd(1 1 1) surface, but the adsorption of NO on a Pd monolayer at 95 K is completely different.

Annealing studies using HREELS show a temperature dependence for the 1744 cm^{-1} HREELS loss peak that corresponds to the desorption of N_2O observed in TPD studies. We propose that the new adsorption state of NO formed on the Pd monolayer film at 95 K is the precursor to N_2O formation.

We identify this species by comparing our results to data for NO adsorbed on Ag(1 1 1) [34]. N_2O is formed in that system at low temperatures from an NO dimer $(NO)_2$ precursor which is stable to 90 K. Bands in RAIRS at 1863 and 1788 cm^{-1} arise from the symmetric and asymmetric NO stretching modes, respectively, of adsorbed $(NO)_2$. As shown in the inset in Fig. 3, two peaks in the spectra from the Pd monolayer are at similar energies to the NO dimer bands observed in RAIRS from Ag(1 1 1). Then, the 1594 cm^{-1} loss peak can be assigned to bridge-bonded NO much like that on the bulk Pd(1 1 1) surface.

One difference, however, is that the dominant energy loss peak on the Pd monolayer occurs at 1744 cm^{-1}, which is close in energy to the asymmetric mode on Ag(1 1 1). Only an "end-on" geometry

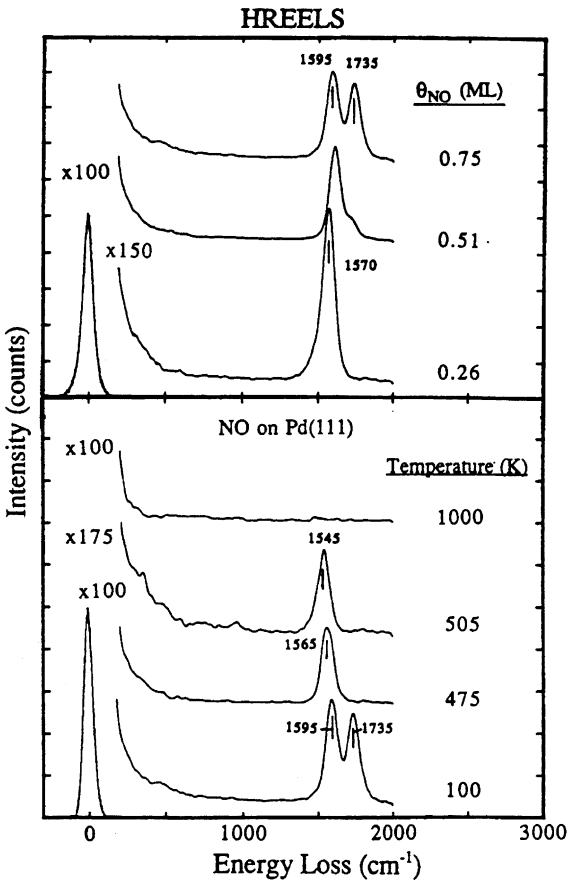

Fig. 6. HREELS spectra for NO at several coverages on Pd(1 1 1) at 95 K (top), and for a saturation coverage after heating to the specified temperature (bottom).

for the dimer can give rise to this mode because of the dipole selection rule for specular scattering in HREELS. In an end-on geometry, both modes are allowed. The NO dimer at monolayer coverage on Ag(1 1 1) is oriented with the N–N bond parallel to the surface plane with the NO groups tilted by 30° [34]. In this orientation, only the symmetric mode is observed at 1863 cm^{-1}.

3.1.3. LEED observations following NO exposure

The beat pattern in LEED for the $\theta_{Pd} = 1$ film at 95 K was visible for NO exposures up to 1.2 L, but the background intensity increased with NO exposure. Larger exposures eventually caused the beat spots to fade. No other ordered patterns were observed and the beat spots reappeared after heating to 400 K. This is different from the case of CO adsorption on the Pd monolayer which reversibly reconstructed the fcc(1 1 1) structure at 95 K to form the pseudomorphic bcc(1 1 0) Pd monolayer with a weak (1 × 1) pattern [12].

3.2. NO adsorption on ultrathin Pd films of increasing thickness

TPD was used to probe adsorption and reaction of NO on Pd films of varying thickness ($\theta_{Pd} = 0.7$, 1, 2, 3, and 5 ML). The $\theta_{Pd} = 0.7$ and 1 films correspond to Pd monolayers with pseudomorphic bcc(1 1 0) and incommensurate fcc(1 1 1) structures, respectively. Exposures of 0.54 and 0.84-L NO produced intermediate coverages of 0.43 and 0.68 ML NO respectively.

NO and N_2O TPD spectra shown in Fig. 7 were obtained following 0.54-L NO exposures on several Pd films at 95 K. Fig. 7a shows a single NO desorption peak at 135 K on the $\theta_{Pd} = 0.73$, 1 and 2 films that is primarily due to cracking of N_2O in the QMS. However, with an increase in film thickness to $\theta_{Pd} = 3.2$, high temperature, molecular NO desorption occurs. From a $\theta_{Pd} = 5$ film, NO desorption, in a peak at 484 K with a small shoulder near 350 K, closely resembles that from a bulk Pd(1 1 1) sample for a similar NO coverage (see Fig. 3). N_2O desorbed in a single peak at 135 K on the $\theta_{Pd} = 0.73$ film as shown in Fig. 7b. The amount of N_2O desorption increased for the $\theta_{Pd} = 1$ film, but then decreased as the Pd film thickness was increased to $\theta_{Pd} = 2$, and then further to $\theta_{Pd} = 3.2$. The N_2O TPD peak temperature did not change. No N_2O desorbed from the $\theta_{Pd} = 5$ film, in agreement with behavior on a bulk Pd(1 1 1) sample.

TPD spectra after 0.84-L NO exposures on several Pd films at 95 K are shown in Fig. 8. The same trends as those in Fig. 7 are evident. TPD spectra from the pseudomorphic ($\theta_{Pd} = 0.71$) and incommensurate ($\theta_{Pd} = 1$) monolayer films are nearly the same, but more N_2O desorbs from the fcc(1 1 1) Pd monolayer than from the pseudomorphic Pd monolayer. NO TPD spectra are dominated at low temperature by N_2O cracking peaks on Pd films up to $\theta_{Pd} = 2.5$. The $\theta_{Pd} = 3$ film

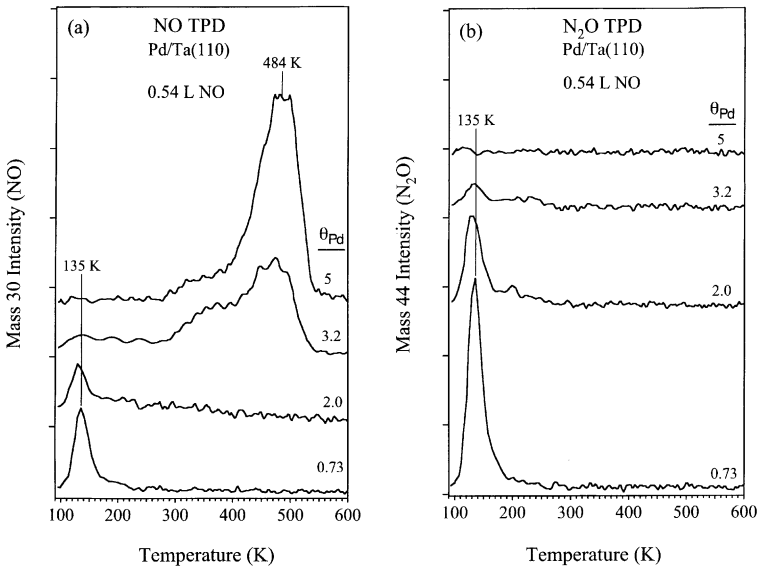

Fig. 7. TPD spectra following 0.54-L NO exposures on Pd films at 95 K: (a) NO TPD spectra (30 amu) and (b) N_2O TPD spectra (44 amu).

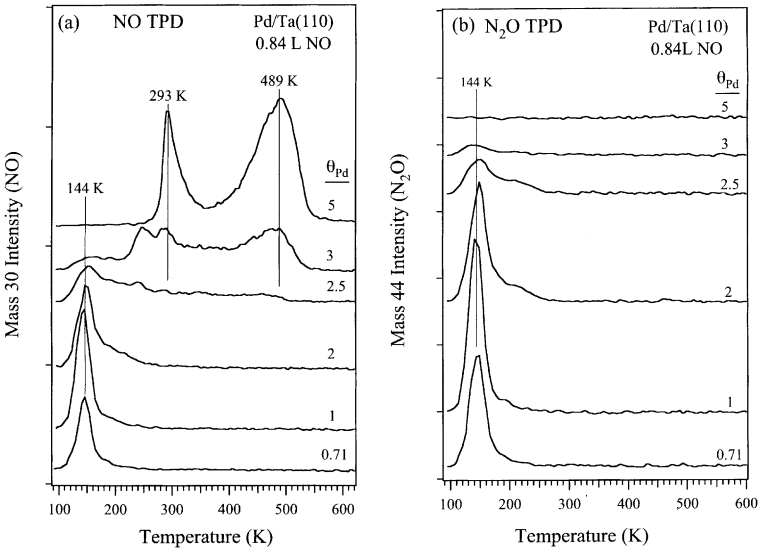

Fig. 8. TPD spectra following 0.84-L NO exposures on Pd films at 95 K: (a) NO TPD spectra (30 amu) and (b) N_2O TPD spectra (44 amu).

shows behavior that is different from that at $\theta_{Pd} = 2$ and 5. On the $\theta_{Pd} = 5$ film, two NO desorption peaks occur that are nearly identical to the NO TPD peaks seen for NO adsorbed on a bulk Pd(1 1 1) surface. N_2O desorption declines as the Pd film thickness increases above $\theta_{Pd} = 1$, and there is no N_2O desorption from the $\theta_{Pd} = 5$ film.

The amount of NO and N_2O desorption as the Pd film thickness is increased can be quantified using the TPD peak areas. Since 0.54 and 0.84-L

exposures of NO show similar general trends, we present only the 0.84-L NO data in Fig. 9. N_2O desorption increased from the fcc(1 1 1) Pd monolayer compared to the bcc(1 1 0) Pd monolayer. This could arise from an increased number of reaction sites available for NO conversion on the monolayer with the higher Pd surface density, or from a lower susceptibility to regions of exposed Ta atoms (e.g., at domain boundaries) which could lead to facile and complete decomposition of NO and thus a reduced product yield. NO has nearly the same chemistry on the Pd bilayer film, $\theta_{Pd} = 2$, as on the Pd monolayers. However, as soon as the Pd thickness exceeds the bilayer film, there is a sharp drop in the yield of desorbed N_2O. This occurs concurrently with increased NO desorption. On a thick $\theta_{Pd} = 5$ film, N_2O desorption is eliminated and NO desorbs in a peak reminiscent of that on a bulk Pd(1 1 1) surface (Fig. 2). On ultrathin Pd films on Ta, the CO TPD areas remained essentially constant as the film thickness was increased from $\theta_{Pd} = 1$ to 5 for a saturation CO exposure [12].

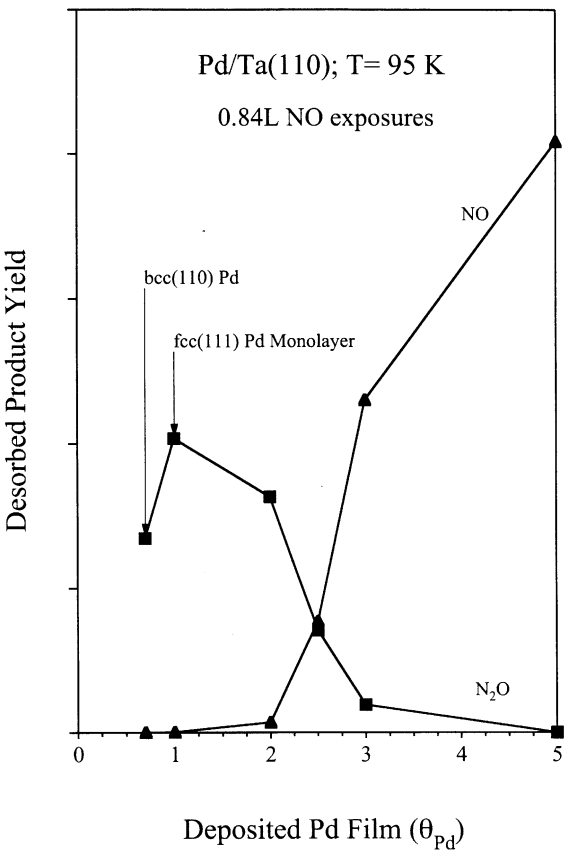

Fig. 9. Desorbed product yields of NO and N_2O after an exposure of 0.84-L NO on Pd films at 95 K.

3.3. NO adsorption on unannealed Pd films deposited on Ta(1 1 0) at 100 K

Previous studies of H_2 and CO chemisorption on Pd films deposited on Ta(1 1 0) have shown significant differences between annealed and unannealed Pd films [6,12]. We also investigated NO adsorption on unannealed Pd films in order to probe differences in the chemical reactivity from annealed Pd films. Unannealed Pd films offer an improved view of the difference in the chemistry of Pd films that have thickness of one layer, two layers, three layers, and so on, because preannealing deposited Pd films to 600 K forms small Pd clusters that are 2–3 layers thick on top of a partially exposed Pd monolayer. Unannealed Pd films are thought to be relatively flat [6,12,36], but will likely have more "defects" than annealed Pd films due to imperfect layering. Other disadvantages of using unannealed films include poorer ordering in the films, changing film structure during heating in TPD, and increased amounts of coadsorbed background gases.

Fig. 10a shows that no NO desorption occurs following 0.54-L NO exposures on unannealed Pd films with $\theta_{Pd} \leqslant 2$ at 95 K. On a $\theta_{Pd} = 3$ film, NO desorbs in a peak at 500 K. Increasing the Pd film thickness to $\theta_{Pd} = 5$ ML nearly doubles the amount of NO desorption without any shift in the desorption temperature. Fig. 10b shows that no N_2O desorption occurs from the $\theta_{Pd} = 0.73$ film, but a small, low-temperature, 44-amu peak was observed at 125 K on thicker films. This peak is due to CO_2 formed by CO oxidation on films thicker than 1 ML (a coincident peak in the 12-amu TPD signal was observed). A much larger concentration of adsorbed CO is present in the unannealed film experiments because CO accumulates during Pd evaporation and characterization of the films using AES, and this is not

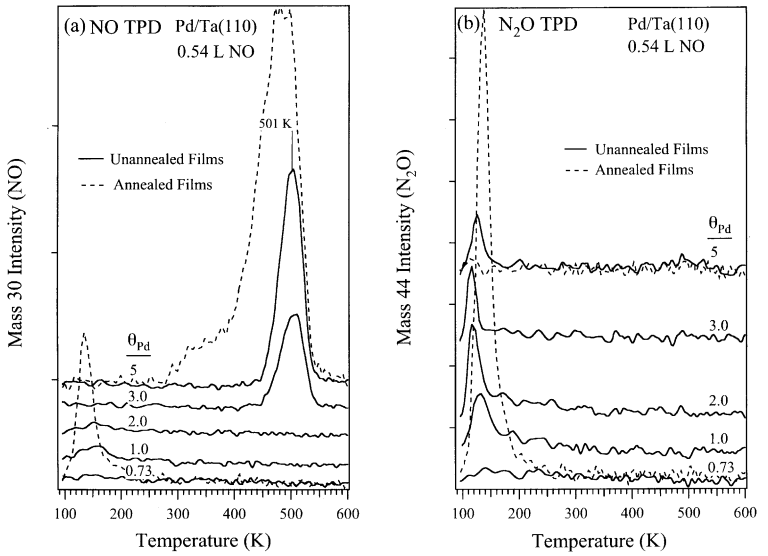

Fig. 10. TPD spectra following 0.54-L NO exposures on unannealed Pd films at 95 K. Desorption curves from annealed Pd films are shown as dashed lines for comparison.

driven off by preannealing prior to NO dosing. Evidently, small NO coverages, diminished by the site-blocking effects of preadsorbed CO, readily oxidize CO to CO_2.

Fig. 10 also includes a reproduction of the TPD spectra from annealed films with $\theta_{Pd} = 0.73$ (bottom dashed curve) and $\theta_{Pd} = 5$ (top dashed curve), to enable a direct comparison with the results in Fig. 7. This further supports the conclusion that a $\theta_{Pd} = 5$ film has bulk-like Pd properties but that a large change occurs in the chemical properties of ultrathin films at or below two-layers thick. The difficulties with coadsorbate contamination in working with unannealed films, as explained above, is also apparent.

3.4. N_2O chemisorption on Pd films

N_2O adsorption on two Pd films, with $\theta_{Pd} = 1$ and 5, was investigated to gain information about the kinetics of N_2O formation from reactions of NO and to further probe the reactivity of these films. Fig. 11 shows N_2O TPD spectra following large (saturation) exposures of N_2O on preannealed Pd films at 95 K. On both the $\theta_{Pd} = 1$ and 5 films, N_2O reversibly adsorbs and desorbs in a single, low temperature peak near 115 K. The small, broad feature near 190 K is due to desorption from Ta, as confirmed by experiments performed on clean Ta(1 1 0). Signals at several other masses, including 30 and 28 amu, were also monitored and these results support the above conclusions. N_2O adsorbs weakly on Pd and no N_2O adsorption occurred on bulk-terminated Pd(1 1 1) at 100 K [27].

The N_2O TPD spectra in Fig. 11 also prove that the rate-limiting step for the desorption of N_2O in TPD following NO exposures is not N_2O desorption, but rather some surface reaction that forms N_2O. N_2O evolution following a saturation NO exposure on the $\theta_{Pd} = 1$ film (bottom curve), occurs at a temperature 45 K higher than that required for N_2O desorption from an adsorbed N_2O monolayer.

HREELS spectra following N_2O adsorption on the fcc(1 1 1) Pd monolayer are shown in Fig. 12. The energy loss peaks at 556, 1284, and 2228 cm^{-1} correspond well to those from an N_2O multilayer on Pt(1 1 1), with loss peaks at 590, 1300 and 2230 cm^{-1} [41]. Thus, N_2O adsorbs molecularly on the $\theta_{Pd} = 1$ film. Furthermore, this spectrum proves that there are no adsorbed N_2O energy loss peaks following NO adsorption on the fcc(1 1 1)-Pd ML at 95 K prior to TPD. This supports the

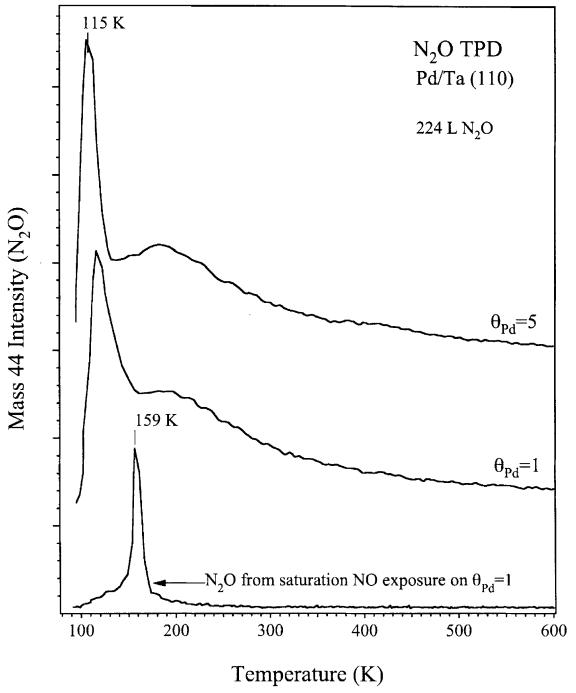

Fig. 11. N_2O TPD spectra following 224-L N_2O exposures on $\theta_{Pd} = 1$ and $\theta_{Pd} = 5$ films at 95 K (top two curves). N_2O desorption from a NO monolayer on the $\theta_{Pd} = 1$ film is shown as the bottom curve.

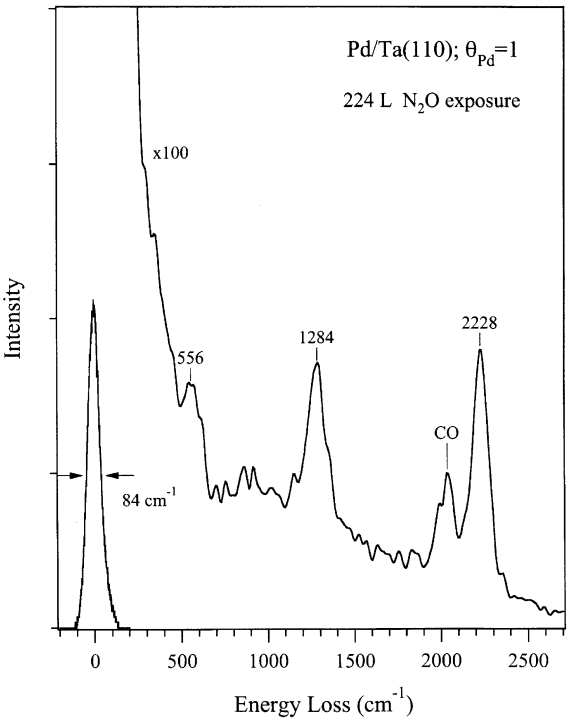

Fig. 12. HREELS spectra following a 224-L N_2O exposure on the fcc(1 1 1) Pd monolayer at 95 K.

conclusion that some precursor is formed prior to desorption of N_2O from the Pd monolayer.

4. Discussion

The adsorption and reaction of NO on monolayer and bilayer Pd films on Ta(1 1 0) is quite different from NO chemisorption on thicker Pd films or on bulk Pd, single-crystal surfaces. We begin our discussion of this altered chemistry with a comparison between the properties of the incommensurate fcc(1 1 1) Pd monolayer with $\theta_{Pd} = 1$ on Ta(1 1 0) and (1 1 1) surfaces of bulk Pd substrates.

On the Pd monolayer at 95 K, NO adsorbs molecularly at low coverages, forming a surface-bound NO dimer species $(NO)_2$ in the adsorbed layer. This species is a precursor to N_2O formation which decomposes to evolve N_2O in a reaction-limited desorption peak in TPD. Some NO desorption also occurs at high coverages. On Pd(1 1 1), however, NO is molecularly chemisorbed at bridging sites up to $\theta_{NO} = 0.5$ and at both atop and bridging sites at monolayer coverage. NO is completely reversibly adsorbed and this surface shows no propensity for NO reaction or dissociation.

The adsorption energy of NO is further evidence of this altered chemistry. On the bulk-terminated Pd(1 1 1) surface, Pd–NO bond strengths are 38, 21, and 20 kcal/mol [27]. In contrast, the Pd–NO bond on the Pd monolayer is just 8 kcal/mol, a reduction of 60% from even the most weakly bound state on Pd(1 1 1).

The principle origin of the altered chemisorption properties of the $\theta_{Pd} = 1$ film are not due to morphological imperfections such as surface roughness or step-like defects in the Pd film. Schmick and Wassmuth [42] studied NO adsorption on a stepped Pd(1 1 1) surface which was inclined 3° to the

(1 1 1) face. They observed decomposition of NO, which was attributed to reactions at step sites, and observed NO, N_2O and N_2 desorption products. However, the N_2O and N_2 products desorbed at temperatures above 400 K in contrast to the N_2O evolution at 160 K on the Pd films.

Another key comparison to make is to NO chemistry on other crystal faces of bulk Pd, single-crystal substrates, such as Pd(1 0 0) and Pd(1 1 0) [43,44]. This provides some insight into the role that may be played by alterations in the geometric structure of the Pd monolayer. NO decomposition was observed on Pd(1 0 0), but the reaction products were evolved only at temperatures exceeding 500 K. An NO dimer was assigned at high coverage on Pd(1 1 0), and a vibrational band at 1694 cm^{-1} was correlated with a desorption peak at 270 K. Extensive surface reconstruction was also proposed to occur. However, the reaction of this species is different from the NO dimer formed on the Pd monolayer, where N_2O was produced in high yield and at 129–159 K. Thus an altered Pd geometry/symmetry does not completely explain the altered reactivity of the Pd monolayer film.

This leaves modification of the electronic structure of Pd that arises from direct interaction with the substrate or lattice strain as the principle driving force for the unique chemistry of the Pd monolayer film. It is of particular interest for understanding the changes that occur in the Pd film electronic structure to compare the Pd film chemistry to that on Rh [45] and Ag [32–34] surfaces. In different limits of bonding interactions between Pd and Ta, changes in the 4d valence-level electron density by charge transfer and/or rehybridization may cause Pd to more nearly resemble Rh or Ag. Comparisons of the NO chemistry on Pd films with that on Rh and Ag surfaces should constrain possible theories on the origins of the altered Pd film properties.

NO decomposes on both Rh(1 1 1) [45] and Ag(1 1 1) surfaces [32–34]. In the case of Rh(1 1 1), desorption of NO, O_2 and N_2 occurs at temperatures above 400 K. No N_2O desorption was observed. In contrast, on Ag(1 1 1), NO, N_2O and N_2 products are formed which are desorbed below 200 K along with an O_2 product which desorbs at 510 K. There are a number of similarities between the adsorption and reaction of NO on a Ag(1 1 1) surface and on the $\theta_{Pd} = 1$ film on Ta(1 1 0), and a more detailed comparison of the two surfaces is warranted.

NO desorbs in a peak at 100 K after low NO exposures on a Ag(1 1 1) surface [32,33]. At higher exposures, this peak shifted 13 K higher and a new NO desorption peak appeared at 90 K along with much smaller peaks at 190 and 400 K. After large NO exposures, N_2O desorbed in peaks at the same temperatures as the low-temperature NO peaks at 90 and 113 K. Ag(1 1 1) and the Pd monolayer initially show single, low temperature peaks for NO and N_2O desorption which shift up in temperature with NO coverage. A second NO desorption peak occurs at lower temperatures on both surfaces at higher coverages. However, the N_2O spectrum from the Pd monolayer has no additional low temperature peak and no NO desorption occurs at 190 or 400 K.

HREELS data for NO adsorption on Ag(1 1 1) [33] also has similarities to our results on the $\theta_{Pd} = 1$ film. Loss peaks were observed at 234, 363, 1153, and 1282 cm^{-1} for small NO exposures on Ag(1 1 1). These were assigned to ν_{Ag-NO}, ν_{Ag-N}, and ν_{NO} for bridge-bonded bent NO, and ν_{NO} for bridge-bonded linear NO, respectively. Small exposures of NO on the $\theta_{Pd} = 1$ film on the Ta(1 1 0) surface gave rise to loss peaks at 322, 1588 and 1690 cm^{-1} which were assigned to ν_{Pd-NO} and two ν_{NO} modes for NO adsorbed at bridge-bonded sites. Large NO exposures on Ag(1 1 1) led to new losses at 1750, 1879 and 2258 cm^{-1} that were attributed to ν_{NO} of NO adsorbed in bent and linear atop sites and to the N–N stretch of N_2O respectively. Large NO exposures on the $\theta_{Pd} = 1$ film lead to losses at 1594, 1744, and 1879 cm^{-1} that were assigned to ν_{NO} and to the asymmetric and symmetric NO-stretching modes of a NO dimer.

An isotopic RAIRS study by Brown et al. [34] on Ag(1 1 1) offered alternative assignments for the previous HREELS results [33]. Loss peaks at 1252 and 2233 cm^{-1} were assigned to adsorbed N_2O and peaks at 1863 and 1788 cm^{-1} were determined to result from the symmetric and asymmetric NO-stretching modes of a NO species. This change in interpretation of the NO chemistry on Ag(1 1 1) makes it very similar to that on the Pd monolayer

film. The primary difference is that no N_2O vibrational modes were observed, and thus no N_2O product is stable on the Pd monolayer. This is because $(NO)_2$ is more stable on the Pd monolayer and N_2O formation is rate-limited by decomposition of the dimer at 160 K and then it desorbs immediately. On Ag(1 1 1), N_2O formation occurs at 70–90 K and then N_2O remains bound at the surface until it desorbs at 115 K.

The pseudomorphic bcc(1 1 0) Pd monolayer and incommensurate fcc(1 1 1) Pd monolayer have identical NO chemistry except for an increase in N_2O yield on the dense, incommensurate Pd layer. The $\theta_{Pd} = 2$ film also has chemistry that closely resembles the $\theta_{Pd} = 1$ film. The most significant difference is a decrease in the amount of N_2O and NO desorption. This is probably because of an increased reactivity of the surface and the accumulation of tightly bound, adatom products. However, a large change occurs for a Pd film thickness of $\theta_{Pd} = 3$. For this film, the propensity for reversible NO adsorption increases dramatically and high temperature, NO desorption peaks appear that reproduce those from bulk Pd(1 1 1) single crystals. In annealed films, a significant amount of the Pd monolayer is available for adsorption and reaction because of morphology changes that occur during annealing that create a range of thicknesses for these Pd films. This accounts for the low temperature N_2O desorption. By $\theta_{Pd} = 5$, NO has no access to the Pd monolayer or bilayer, and the properties of this film are identical to bulk Pd(1 1 1) surfaces with respect to NO chemisorption and reaction.

Access of NO to the Pd monolayer is more quickly eliminated with increasing deposited-film thickness for unannealed Pd films. But, increased concentrations of surface imperfections cause the amount of desorbing N_2O to be much less than that from the annealed Pd films. N_2O desorption from unannealed films with $\theta_{Pd} > 1$ is negligible. This illustrates how quickly the altered chemisorption properties drop off with Pd film thickness. Less NO desorbs from the unannealed $\theta_{Pd} = 5$ film than from the annealed film because improved ordering of the thick film surface by preannealing greatly increases the propensity for reversible adsorption.

NO chemisorption on the Pd monolayer on Ta(1 1 0) resembles that on the Ag(1 1 1) surface, including low-temperature NO dimer formation and N_2O desorption. Ag carries out facile formation of a NO dimer which leads to formation of N_2O at very low temperatures [32–34]. These observations support conclusions that Pd interaction with Ta(1 1 0) results in filling of the Pd d-band, producing an electronic structure and reactivity similar to that of Ag. Because of the similarities of the pseudomorphic and incommensurate monolayers and the Pd bilayer film, lattice strain appears to play a less important role than direct Pd–Ta bonding interactions that lead to rehybridization and charge transfer. (Unless there is a critical lattice strain beyond which no further change occurs.)

Finally, we compare the chemistry of NO and CO on these Pd films. The molecular orbital structure of NO is the same as that for CO except for an additional electron in the 2π orbital of free NO. This makes the NO ligand a weaker π-acid (electron acceptor) and a more versatile ligand than CO because of the possibility of forming a covalent bond to the surface with the unpaired 2π electron. CO adsorbs on a $\theta_{Pd} = 1$ film on Ta(1 1 0) with an adsorption energy of 15 kcal/mol [4,13,36]. This is almost 40% lower than that observed on Pd(1 1 1) (36 kcal/mol) [27,46] or on Pd(1 0 0) surfaces (38.5 kcal/mol) [47,48]. The adsorption energy of NO is also strongly reduced on a $\theta_{Pd} = 1$ film on Ta(1 1 0) to 8 kcal/mol, which is only about 21% of that observed on Pd(1 1 1) (38 kcal/mol) or on Pd(1 0 0) (30 kcal/mol) surfaces [30]. Adsorption of CO on Pd films on Ta(1 1 0) was completely reversible, indicating that "defects" are not dominating the observed chemistry.

5. Conclusions

NO and N_2O chemisorption reveals new insight into the chemisorption properties of ultrathin Pd films deposited on Ta(1 1 0). The desorption energy of NO is greatly reduced to only 8 kcal/mol on Pd monolayer ($\theta_{Pd} = 0.76$ and 1) and bilayer ($\theta_{Pd} = 2$) films. NO adsorption on these films at 95 K leads to the formation of a NO dimer which

decomposes at 140–160 K to yield N_2O desorption peaks in TPD. These data show that the interaction of NO with the Pd monolayer and bilayer films resembles that for a Ag(1 1 1) surface in many respects. Thus, the chemistry that we observe for NO adsorbed on the Pd monolayer and bilayer can be explained by a completely filled Pd d band resulting primarily from charge transfer and/or rehybridization of Pd to an electronic structure similar to Ag. The surface reactivity of thicker Pd films rapidly evolves to that of bulk Pd(1 1 1) surfaces, with some additional "tuning" of the NO chemisorption properties possible only for Pd films in the thickness range of 2–3 layers. NO chemisorption on Pd films that are five-layers thick is identical to that on bulk Pd(1 1 1) surfaces.

Acknowledgements

Support of this work by the Analytical and Surface Chemistry Program in the Division of Chemistry of the National Science Foundation is acknowledged. We wish to thank Professor Myron Strongin for loan of the Ta(1 1 0) crystal.

References

[1] H. Poppa, F. Soria, Phys. Rev. B 27 (1983) 5166.
[2] D.L. Neiman, B.E. Koel, in: D.M. Zehner, D.W. Goodman (Eds.), Physical and Chemical Properties of Thin Metal Overlayers and Alloy Surfaces, Materials Research Society, Pittsburgh, PA, 1988, p. 143.
[3] P.J. Berlowitz, D.W. Goodman, Langmuir 4 (1988) 1091.
[4] B.E. Koel, R.J. Smith, P.J. Berlowitz, Surf. Sci. 231 (1990) 325.
[5] J.M. Heitzinger, S.C. Gebhard, B.E. Koel, Chem. Phys. Lett. 200 (1992) 65.
[6] J.M. Heitzinger, A. Avoyan, B.E. Koel, Surf. Sci. 294 (1993) 251.
[7] D. Prigge, W. Schlenk, E. Bauer, Surf. Sci. 123 (1982) L698.
[8] M.W. Ruckman, P.D. Johnson, M. Strongin, Phys. Rev. B 31 (1985) 3405.
[9] M.W. Ruckman, M. Strongin, Phys. Rev. B 29 (1984) 7105.
[10] J.M. Heitzinger, S.C. Gebhard, B.E. Koel, Surf. Sci. 275 (1992) 209.
[11] Y.B. Zhao, R. Gomer, Surf. Sci. 239 (1990) 189.
[12] A. Sellidj, B.E. Koel, Surf. Sci. 284 (1993) 139.
[13] W.K. Kuhn, J. Szanyi, D.W. Goodman, Surf. Sci. 303 (1994) 377.
[14] S.-L. Weng, M. El-Batanouny, Phys. Rev. Lett. 44 (1980) 612.
[15] M. El-Batanouny, M. Strongin, G.P. Williams, J. Colbert, Phys. Rev. Lett. 46 (1981) 269.
[16] G.P. Williams, M. El-Batanouny, J. Colbert, E. Jensen, T.N. Rhodin, Phys. Rev. B 25 (1982) 3658.
[17] M. El-Batanouny, D.R. Hamann, S.R. Chubb, J.W. Davenport, Phys. Rev. B 27 (1983) 2575.
[18] X. Pan, P.D. Johnson, M. Weinert, R.E. Watson, J.W. Davenport, G.W. Fernando, S.L. Hulbert, Phys. Rev. B 38 (1988) 7850.
[19] V. Kumar, K.H. Bennemann, Phys. Rev. B 28 (1983) 3138.
[20] J.A. Rodriguez, R.A. Campbell, D.W. Goodman, J. Vac. Sci. Technol. A 10 (1992) 2540.
[21] B.A. Banse, B.E. Koel, Surf. Sci. 232 (1990) 275.
[22] G.K. Wertheim, J.E. Rowe, J.A. Rodriquez, D.W. Goodman, Science 260 (1993) 1527.
[23] G.K. Wertheim, D.N.E. Buchanan, Phys. Rev. B 40 (1989) 5319.
[24] M.W. Ruckman, L.Q. Jiang, M. Strongin, J. Vac. Sci. Technol. A (1992) 2551.
[25] M.E. Bartram, B.E. Koel, E.A. Carter, Surf. Sci. 219 (1989) 467.
[26] C. Nyberg, P. Uvdal, Surf. Sci. 219 (1989) 467.
[27] D.T. Wickham, B.A. Banse, B.E. Koel, Surf. Sci. 243 (1991) 83.
[28] M. Bertolo, K. Jacobi, Surf. Sci. 226 (1990) 207.
[29] H. Conrad, G. Ertl, J. Kuppers, E.E. Latta, Surf. Sci. 65 (1977) 235.
[30] S.W. Jorgensen, N.D.S. Canning, R.J. Madix, Surf. Sci. 179 (1987) 322.
[31] A. Sandell, A. Nilsson, N. Martensson, Surf. Sci. 241 (1991) L1.
[32] R.J. Behm, C.R. Brundle, J. Vac. Sci. Technol. A 2 (1984) 1040.
[33] S.K. So, R. Franchy, W. Ho, J. Chem. Phys. 91 (1989) 5701.
[34] W.A. Brown, P. Gardiner, D.A. King, J. Phys. Chem. (1995) 7065.
[35] R.G. Windham, M.E. Bartram, B.E. Koel, J. Phys. Chem. 92 (1988) 2862.
[36] A. Sellidj, B.E. Koel, Surf. Sci. 281 (1993) 223.
[37] M. Sagurton, M. Strongin, F. Jona, J. Colbert, Phys. Rev. B 28 (1983) 4075.
[38] M. Strongin, M. El-Batanouny, M.A. Pick, Phys. Rev. B 22 (1980) 3126.
[39] M.W. Ruckman, V. Murgai, M. Strongin, Phys. Rev. B 34 (1986) 6759.
[40] P.A. Redhead, Vacuum 12 (1962) 203.
[41] N.R. Avery, Surf. Sci. 131 (1983) 501.
[42] H.D. Schmick, H.-W. Wassmuth, Surf. Sci. 123 (1982) 471.
[43] C. Nyberg, P. Uvdal, Surf. Sci. 204 (1988) 517.
[44] R. Raval, M.A. Harrison, S. Haq, D.A. King, Surf. Sci. 294 (1993) 10.

[45] T.W. Root, L.D. Schmidt, G.B. Fisher, Surf. Sci. 134 (1983) 30.
[46] X. Guo, J.T. Yates Jr., J. Chem. Phys. 90 (1989) 6761.
[47] J.C. Tracy, P.W. Palmberg, Surf. Sci. 14 (1969) 274.
[48] R.J. Behm, K. Christmann, G. Ertl, M.A. Van Hove, J. Chem. Phys. 73 (1980) 2984.